Thermal vapor sulfurization of molybdenum layers

María J. Hortigüela*, Igor Bdikin, Gonzalo Otero-Irurueta*

[a] Nanoengineering Research group, Centre for Mechanical Technology & Automation, University of Aveiro, 3810-193 Aveiro, Portugal

ARTICLE INFO

ABSTRACT

Sulfurization of molybdenum layers is a promising route for obtaining large-scale and high-quality transition metal dichalcogenides. Here we describe the synthesis of continuous and homogeneous MoS_2 in the centimeter scale by the thermal vapor sulfurization of pre-deposited molybdenum precursors on SiO_2. Metallic molybdenum as well as MoO_3 were used as precursors while the sulfurization was performed by chemical vapor deposition. A multi-technique characterization was employed to fully describe the deposition of molybdenum as well as its sulfurization. Thus, Raman spectroscopy, X-ray and ultra-violet photoelectron spectroscopies as well as scanning electron and atomic force microscopies indicated that the molybdenum layers were completely transformed in MoS_2. The samples were homogeneous in the centimeter scale and quite flat with a root mean square roughness of 1.4 Å. Furthermore, its work function was 4.1 eV.

1. Introduction

Transition Metal Dichalcogenides (TMDs) are attracting a wide range of research interest due to its unique properties and possible applications [1–3]. Thus, these 2D materials, combined with others or functionalized, can be employed in several fields such as catalysis [4], solar cells [5] and nano-electronics [2,6–7].

In particular, MoS_2 is the most popular TMD. There are several methods for synthesizing it, being the most extended mechanical and chemical exfoliation and chemical vapor deposition (CVD) [1,2]. Each of these methods has several advantages and drawbacks. The main advantage of exfoliation is to produce free-standing MoS_2 layers that could be used in different applications and devices. Nevertheless, this methodology produce low quality samples [2] with a high level of defects. Moreover, the size, shape and thick of the MoS_2 flakes is not well controlled by this methodology [2]. On the other hand, standard CVD synthesize MoS_2 on relevant substrates such as SiO_2 [2,8,9] and sapphire [9,10]. The main advantage of CVD is the high quality of the samples in comparison with that obtained by exfoliation [8]. Nevertheless, standard CVD use to produce inhomogeneous or discontinuous films in which high quality MoS_2 was found only in small regions of the substrate [8].

Thus, a large effort is still necessary for obtaining high quality, large area and continuous samples that can be used in the proposed applications in a reproducible way. In the search of new approaches for obtaining those kind of samples, it was recently showed that the pre-adsorption of molybdenum species on a substrate followed by its sulfurization is a much better method than standard CVD [2,11–13]. In this context, it is clear that both the molybdenum rich precursor as well as the method for its pre-deposition can influence the quality of the MoS_2 samples. Thus, Mo, MoO_3, $MoCl_5$, $Mo(CO)_6$ [14] and others [2] were tested as molybdenum precursors, while the deposition was performed by electron-beam [15], magnetron-sputtering, pulsed-laser deposition, atomic layer deposition and thermal evaporation [14]. These deposition methods have the advantage of well controlling the molybdenum rich layer that are sulfurized in a second step and thus, they use to produce high quality MoS_2 with the desired shape and thick.

In this paper, metallic Mo and MoO_3 are pre-deposited on SiO_2 by thermal evaporation under vacuum conditions. Then, the molybdenum layers are transformed in high quality MoS_2 by thermal vapor sulfurization. Moreover, MoS_2 samples are thoroughly characterized by a combination of several experimental techniques including X-ray and Ultra Violet photoelectron spectroscopies (XPS and UPS), Scanning Electron Microscopy (SEM), Atomic Force Microscopy (AFM) and Raman Spectroscopy.

2. Experimental details

SiO_2 substrates were cleaned by acetone and ethanol in an ultrasonic system. Before molybdenum deposition they were checked by XPS and UPS. The size of the substrates used in this work ranged from 1×0.5 cm^2 to 1×1 cm^2.

In the case of the thermal evaporation of Mo, it was used a Mo wire with a diameter of 0.25 mm while 5.2 A of electrical current was

---

* Corresponding authors.
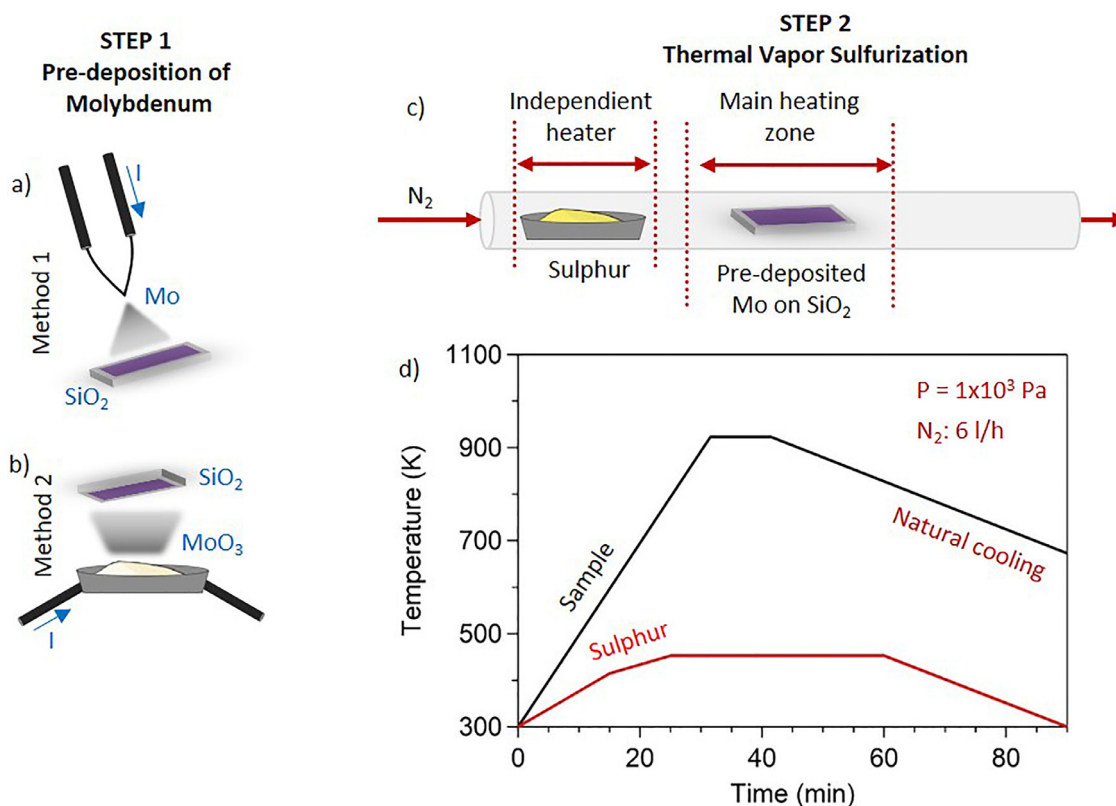*E-mail addresses:* mhortiguela@ua.pt (M.J. Hortigüela), otero.gonzalo@ua.pt (G. Otero-Irurueta).

Fig. 1. (a) and (b) representation of the experimental set-up used for depositing molybdenum on SiO₂. (c) Schematic representation of the set up used for the thermal vapor sulfurization of the samples. (d) Temperature vs time ramps of both the sample and the sulfur.

enough for its sublimation at a pressure of 10^{-6} Pa. On the other hand, a nickel boat was used as container for the sublimation of MoO_3 powder. This powder was sublimated at a temperature of 853 K and under a pressure of 0.2 Pa.

XPS spectra were acquired in an Ultra High Vacuum (UHV) system with a base pressure of 2×10^{-8} Pa. The system is equipped with a hemispherical electron energy analyzer (SPECS Phoibos 150), a delay-line detector and a monochromatic AlKα (1486.74 eV) X-ray source. High resolution spectra were recorded at normal emission take-off angle and with a pass-energy of 20 eV, which provides an overall instrumental peak broadening of 0.5 eV. UPS was performed in the same system but by using a He I (21.2 eV) UV lamp. Its resolution is slightly better than 150 mV.

SEM micrographs were obtained on a TM4000Plus microscope (Hitachi). The micrographs were recorder by a backscatter electrons detector for high contrast.

AFM measurements were carried out using a Veeco AFM Multimode Nanoscope (IV) MMAFM-2, Veeco microscopy. A conductive Si cantilever (Nanosensors, nominal force constant of 42 N/m, resonant frequency of 330 kHz) was used. AFM scanning in tapping mode were performed on various parts of the films, which produced reproducible images similar to those displayed in this work.

Micro-Raman spectroscopy was performed using a Jobin Yvon (HORIBA) HR800 instrument, using a 442 nm laser wavelength as excitation source (He:Cd laser, Kimmon, IK series, Japan) and x100 objective (NA = 0.9, Olympus, Japan).

3. Results and discussion

MoS_2 layers were obtained by thermal vapor sulfurization of pre-deposited molybdenum [13,14]. This is a two-step process. Firstly, a desired quantity of molybdenum was deposited on SiO₂ under vacuum conditions and then, the samples were sulfurized in a CVD system under

a sulfur rich atmosphere [2]. The deposition of molybdenum species directly on SiO₂ was performed by two different methods schematically represented in Fig. 1a-b. In the first set up (method 1), an electrical current circulated through a Mo filament producing its annealing and, after reaching the threshold temperature, the sublimation of Mo. This deposition of Mo was performed under ultra-high vacuum conditions for minimizing its oxidation. By positioning the sample just in front of the filament, it was possible to deposit a Mo film of the desired thick. On the other hand, the second method (method 2) consisted in a nickel boat or crucible fulfilled with MoO_3 powder heated by flowing an electrical current. Its temperature was monitored by a thermocouple directly bonded to its center. In both methods, the quantity of molybdenum on the surface was controlled by controlling the evaporation time.

After depositing the molybdenum layer on SiO₂, the samples were thermally vapor sulfurized (TVS) in a chemical vapor deposition system as it is schematically represented in Fig. 1c. An alumina boat containing sulfur powder was mounted at the inlet corner of the quartz tube and independently heated with a heating tape. Importantly, with this configuration it was possible to control the temperature of both the sample and the sulfur as a function of the time. Fig. 1d shows the ramps of temperature vs time used for the thermal vapor sulfurization of the samples. The samples and sulfur powder were heated at maximum temperatures of 930 K and 450 K, respectively. In our experiments, 930 K was the best temperature for fully sulfurizing the Mo layers while heating sulfur at 450 K produces a large excess of S during the experiment. The sulfurization was performed under a N₂ flow of 6 L/h at a pressure of 1×10^3 Pa.

The deposition of Mo from the filament (method 1) was followed by *in situ* XPS, *i.e.* without exposing the sample to atmospheric conditions. Fig. 2a shows the evolution of Mo 3d core level as a function of the evaporation time. Mo $3d_{5/2}$ and Mo $3d_{3/2}$ core levels appeared at binding energies (BEs) of 228 eV and 231.1 eV, respectively, values that
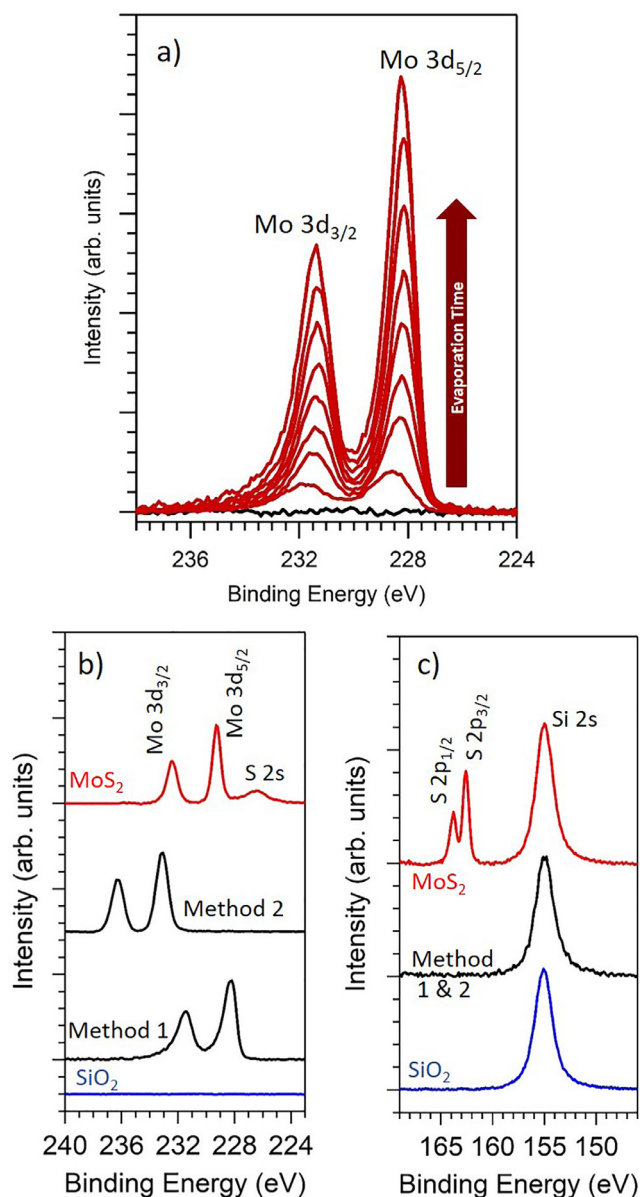
Fig. 2. XPS spectra of clean SiO_2 and the films obtained before and after TVS. (a) Evolution of Mo 3d core level as a function of the evaporation time. (b) Mo 3d and S 2s region. (c) S 2p and Si 2s region.

Fig. 3. (a) SEM image, (b) AFM topographic image and (c) Raman spectra of MoS_2 on SiO_2 obtained at different regions of the sample. a) (450 μm × 400 μm) and b) (5 μm × 5 μm). The inset in (a) shows a photo of the MoS_2 sample in which the cover and uncover regions are clearly distinguished.

are in good agreement with metallic molybdenum [16]. Moreover, the figure shows the ability of this set up for fine-tuning the quantity of Mo deposited on the surface from very low coverages (bottom spectra).

Comparing the evolution of the samples synthesized by both methods, Fig. 2b and c show the XPS regions corresponding to Mo 3d and S 2s (Fig. 2b) and S 2p and Si 2s (Fig. 2c) for a clean SiO_2, after depositing molybdenum by both methods and after their thermal vapor sulfurization. Mo $3d_{5/2}$ core levels peaks from the film deposited by method 1 and 2 appeared at BEs of 228 eV and 232.9 eV, respectively. These values indicate that while the Mo films obtained by method 1 had a metallic character [16], the films obtained by method 2 were oxidized (Mo^{6+}) [16,17]. Complementary, Fig. 2c shows the lack of XPS signal in the S 2p region even after the growth of the Mo films. As it was expected, only the Si 2s core level is detected in this region of the spectra (Fig. 2c, black spectra).

On the other hand, a completely different scenario was obtained after the sulfurization of the samples. Fig. 2b shows a clear change in the XPS signal of Mo 3d core level (red spectra). The two sharp peaks
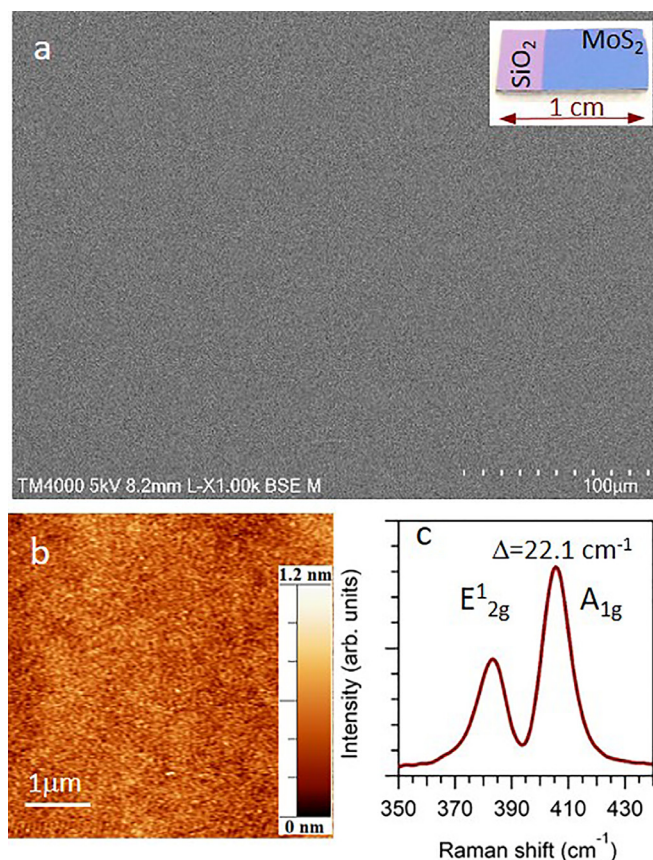
centered at BEs of 229.3 eV (Mo $3d_{5/2}$) and 232.4 eV (Mo $3d_{3/2}$) are in good agreement with the spectra reported for MoS_2 [8,17,18]. Moreover, the new peak detected at a BE of 226.5 eV is ascribed to S 2s core level of MoS_2 samples [8,17,18]. Complementary, the S 2p core level (Fig. 2c, red spectra) showed two sharp components at BEs of 162.2 eV and 163.4 eV, which are ascribed to S $2p_{3/2}$ and S $2p_{1/2}$ in MoS_2 [8,18]. Importantly, in our experiments the quality of the MoS_2 was the same with independence of the method used for depositing the molybdenum layers. Complementary, the topography of the MoS_2 samples was characterized by SEM and AFM as it is showed in Fig. 3a and Fig. 3b, respectively. Moreover, the inset in Fig. 3a shows a photo of the sample in which the cover and uncovered regions are clearly distinguished. The uncovered region on the left is a region masked during the sublimation of molybdenum. The samples obtained by our method were quite homogeneous and continuous in the centimeter scale (Fig. 3a). More in detail, AFM topographic images (Fig. 3b) show an homogeneous sample also in the micro scale. Importantly, the RMS obtained by AFM on this image was only 1.4 Å, in good agreement with previous works. For instance, Lin et al. and Liu et al. reported roughness values of ~2 Å [19] and ~3.4 Å [20], respectively.

Furthermore, Raman spectroscopy was used to reveal the number of layers of the sample. MoS_2 Raman modes E_{2g}^1 and A_{1g} are sensitive to the number of layers, increasing the distance between their frequencies (Δ) with the number of layers and thus, allowing a robust thickness characterization up to 4–5 layers. The Raman spectra of Fig. 3c shows the in-plane (E_{2g}^1) and out-of-plane (A_{1g}) vibration modes at 383.4 and 405.5 cm^{-1}, respectively, values in good agreement with previous works [21–23]. Moreover, the obtained Δ = 22.1 cm^{-1} between the Raman modes indicates a bilayer MoS_2 [21–23].
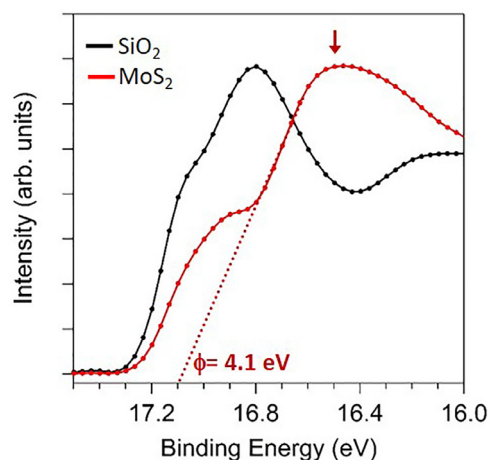
Fig. 4. UPS of SiO_2 and MoS_2. The figure shows the secondary electron cut-off region of the spectra.

Furthermore, UPS can shield some light on the electronic properties of the samples. In this work, it was used for obtaining the work function (ϕ) of the MoS_2 samples. Fig. 4 shows the secondary electron cut-off region of the valence band of clean SiO_2 and MoS_2. The first shoulder, near a BE of 17 eV, was previously ascribed to the SiO_2 substrate [8] while the main peak related with the MoS_2 film is located at a BE of 16.5 eV (red arrow). By linearly extrapolation, it is possible to obtain its work function, which in our case was 4.1 eV, in good agreement with previous reported values [24].

4. Conclusions

Large-area and high-quality MoS_2 was obtained by the thermal vapor sulfurization of pre-deposited molybdenum layers. The results indicated that MoS_2 was uniform and continuous through the SiO_2 substrate in which molybdenum was pre-deposited. Both metallic Mo as well as MoO_3 were completely sulfurized by CVD producing similar results. The obtained samples were quite flat, with a RMS roughness of 1.4 Å while the work function obtained by UPS was 4.1 eV.

5. Acknowledgments

Supplementary materials

Supplementary material associated with this article can be found, in the online version, at doi:10.1016/j.tsf.2019.137588.

References

[1] H. Wang, C. Li, P. Fang, Z. Zhang, J.Z. Zhang, properties Synthesis, and optoelectronic applications of two-dimensional MoS2 and MoS2-based heterostructures, Chem. Soc. Rev 47 (2018) 6101–6127, https://doi.org/10.1039/C8CS00314A.

[2] Y.P. Venkata Subbaiah, K.J. Saji, A. TiwariAtomically Thin MoS 2 , A versatile nongraphene 2D material, Adv. Funct. Mater. 26 (2016) 2046–2069, https://doi.org/10.1002/adfm.201504202.

[3] X. Li, H. ZhuTwo-dimensional MoS2, Properties, preparation, and applications, J. Materiomics 1 (2015) 33–44, https://doi.org/10.1016/j.jmat.2015.03.003.

[4] G. Li, D. Zhang, Q. Qiao, Y. Yu, D. Peterson, A. Zafar, R. Kumar, S. Curtarolo, F. Hunte, S. Shannon, Y. Zhu, W. Yang, L. Cao, All the catalytic active sites of MoS2 for hydrogen evolution, J. Am. Chem. Soc. 138 (2016) 16632–16638, https://doi.org/10.1021/jacs.6b05940.

[5] M.-L. Tsai, S.-H. Su, J.-K. Chang, D.-S. Tsai, C.-H. Chen, C.-I. Wu, L.-J. Li, L.-J. Chen, J.-H. He, Monolayer MoS2 Heterojunction Solar Cells, ACS Nano 8 (2014) 8317–8322, https://doi.org/10.1021/nn502776h.

[6] E. Yalon, C.J. McClellan, K.K.H. Smithe, M. Muñoz Rojo, R.L. Xu, S.V. Suryavanshi, A.J. Gabourie, C.M. Neumann, F. Xiong, A.B. Farimani, E. Pop, Energy dissipation in monolayer MoS2 electronics, Nano Lett. 17 (2017) 3429–3433, https://doi.org/10.1021/acs.nanolett.7b00252.

[7] D. Lembke, S. Bertolazzi, A. Kis, Single-layer MoS2 electronics, Acc. Chem. Res. 48 (2015) 100–110, https://doi.org/10.1021/ar500274q.

[8] D.K. Sharma, E.V. Ramana, S. Fateixa, M.J. Hortigüela, G. Otero-Irurueta, H.I.S. Nogueira, A. Kholkin, Pressure-dependent large area synthesis and electronic structure of MoS2, Mater. Res. Bull. 97 (2018) 265–271, https://doi.org/10.1016/j.materresbull.2017.09.007.

[9] Y. Yu, C. Li, Y. Liu, L. Su, Y. Zhang, L. Cao, Controlled scalable synthesis of uniform, high-quality monolayer and few-layer MoS2 films, Sci. Rep. 3 (2013) 1866, https://doi.org/10.1038/srep01866.

[10] D. Dumcenco, D. Ovchinnikov, K. Marinov, P. Lazić, M. Gibertini, N. Marzari, O.L. Sanchez, Y.-C. Kung, D. Krasnozhon, M.-W. Chen, S. Bertolazzi, P. Gillet, A. Fontcuberta, I. Morral, A. Radenovic, A. Kis, Large-area epitaxial monolayer MoS2, ACS Nano 9 (2015) 4611–4620, https://doi.org/10.1021/acsnano.5b01281.

[11] C.-.R. Wu, X.-.R. Chang, C.-.H. Wu, S.-.Y. Lin, The growth mechanism of transition metal dichalcogenides by using sulfurization of pre-deposited transition metals and the 2D crystal hetero-structure establishment, Sci. Rep. 7 (2017) 42146, https://doi.org/10.1038/srep42146.

[12] H. Liu, K.K. Ansah Antwi, J. Ying, S. Chua, D Chi, Towards large area and continuous MoS2 atomic layers via vapor-phase growth: thermal vapor sulfurization, Nanotechnology 25 (2014) 405702, , https://doi.org/10.1088/0957-4484/25/40/405702.

[13] Y. Shi, H. Li, L.-J. Li, Recent advances in controlled synthesis of two-dimensional transition metal dichalcogenides via vapour deposition techniques, Chem. Soc. Rev. 44 (2015) 2744–2756, https://doi.org/10.1039/C4CS00256C.

[14] H.F. Liu, S.L. Wong, D.Z. Chi, CVD growth of MoS2-based two-dimensional materials, Chem. Vap. Depos 21 (2015) 241–259, https://doi.org/10.1002/cvde.201500060.

[15] S.S. Grønborg, S. Ulstrup, M. Bianchi, M. Dendzik, C.E. Sanders, J.V. Lauritsen, P. Hofmann, J.A. Miwa, Synthesis of epitaxial single-layer MoS2 on Au(111), Langmuir 31 (2015) 9700–9706, https://doi.org/10.1021/acs.langmuir.5b02533.

[16] B. Brox, I. Olefjord, ESCA studies of MoO2 and MoO3, Surf. Interface Anal. 13 (1988) 3–6, https://doi.org/10.1002/sia.740130103.

[17] Y. Lee, J. Lee, H. Bark, I.-K. Oh, G.H. Ryu, Z. Lee, H. Kim, J.H. Cho, J.-H. Ahn, C. Lee, Synthesis of wafer-scale uniform molybdenum disulfide films with control over the layer number using a gas phase sulfur precursor, Nanoscale 6 (2014) 2821, https://doi.org/10.1039/c3nr05993f.

[18] F. Huang, B. Cho, H.-S. Chung, S.B. Son, J.H. Kim, T.-S. Bae, H.J. Yun, J.I. Sohn, K.H. Oh, M.G. Hahm, J.H. Park, W.-K. Hong, The influence of interfacial tensile strain on the charge transport characteristics of MoS2 -based vertical heterojunction devices, Nanoscale 8 (2016) 17598–17607, https://doi.org/10.1039/C6NR05937F.

[19] Y.-.C. Lin, W. Zhang, J.-.K. Huang, K.-.K. Liu, Y.-.H. Lee, C.-.T. Liang, C.-.W. Chu, L.-.J. Li, Wafer-scale MoS2 thin layers prepared by MoO3 sulfurization, Nanoscale 4 (2012) 6637, https://doi.org/10.1039/c2nr31833d.

[20] K.-.K. Liu, W. Zhang, Y.-H. Lee, Y.-C. Lin, M.-.T. Chang, C.-Y. Su, C.-S. Chang, H. Li, Y. Shi, H. Zhang, C.-S. Lai, L.-J. Li, Growth of large-area and highly crystalline Mo2 thin layers on insulating substrates, Nano Lett. 12 (2012) 1538–1544, https://doi.org/10.1021/nl2043612.

[21] C. Lee, H. Yan, L.E. Brus, T.F. Heinz, J. Hone, S. Ryu, Anomalous lattice vibrations of Single- and Few-Layer MoS2, ACS Nano 4 (2010) 2695–2700, https://doi.org/10.1021/nn1003937.

[22] H. Li, Q. Zhang, C.C.R. Yap, B.K. Tay, T.H.T. Edwin, A. Olivier, D Baillargeat, From bulk to monolayer mos2: evolution of Raman scattering, Adv. Funct. Mater. 22 (2012) 1385–1390, https://doi.org/10.1002/adfm.201102111.

[23] S. Najmaei, Z. Liu, W. Zhou, X. Zou, G. Shi, S. Lei, B.I. Yakobson, J.-.C. Idrobo, P.M. Ajayan, J. Lou, Vapour phase growth and grain boundary structure of molybdenum disulphide atomic layers, Nat. Mater. 12 (2013) 754–759, https://doi.org/10.1038/nmat3673.

[24] S.Y. Lee, U.J. Kim, J. Chung, H. Nam, H.Y. Jeong, G.H. Han, H. Kim, H.M. Oh, H. Lee, H. Kim, Y.-G. Roh, J. Kim, S.W. Hwang, Y. Park, Y.H. Lee, Large work function modulation of monolayer MoS2 by ambient gases, ACS Nano 10 (2016) 6100–6107, https://doi.org/10.1021/acsnano.6b01742.